soil systems

MDPI

Article

Evidence of Potential Organo-Mineral Interactions during the First Stage of Mars Terraforming

Beatrice Giannetta [1], Antonio G. Caporale [2], Danilo Olivera de Souza [3], Paola Adamo [2] and Claudio Zaccone [1,4,*]

[1] Department of Biotechnology, University of Verona, Strada Le Grazie 15, 37134 Verona, Italy; beatrice.giannetta@univr.it
[2] Department of Agricultural Sciences, University of Naples Federico II, Via Università 100, 80055 Portici, Italy; ag.caporale@unina.it (A.G.C.); paola.adamo@unina.it (P.A.)
[3] ELETTRA Sincrotrone Trieste S.C.p.A., S.S. 14 Km 163.5, 34149 Trieste, Italy; danilo.olsouza@gmail.com
[4] National Institute of Geophysics and Volcanology, Via Vigna Murata 605, 00143 Roma, Italy
* Correspondence: claudio.zaccone@univr.it; Tel.: +39-045-8027864

Abstract: Future space missions to Mars will depend on the development of bioregenerative life support systems. Mars regolith contains most of the nutrients needed for plant growth, but not organic matter (OM). Although Mars simulants have been deeply characterized and tested as growing media, no data are available about their possible modification occurring during terraforming, including the interaction of exogeneous OM with iron (Fe) oxides, particularly abundant in Mars regolith. The aim of this study was to investigate the mineral transformation and the OM evolution occurring in the early stages of the terraforming process. Potato was grown for 99 days on Mojave Mars Simulant MMS-1, alone (R100) and mixed with a compost 70:30 *v*:*v* (R70C30), and on a fluvial sand, alone (S100) and mixed with compost (S70C30), for comparison. Bulk (BK) and potato tubero/rhizo-sphere (RH) soils were fractionated to obtain particulate OM (POM) and mineral-associated OM (MAOM). Bulk samples and corresponding fractions were characterized for total nitrogen and organic carbon (C) and analyzed by Fe K-edge X-ray absorption near-edge structure (XANES) and extended X-ray absorption fine structure (EXAFS) spectroscopy. Organic C increased by 10 and 25 times in S70C30 and R70C30, respectively, compared to S100 and R100. Most of the organic C accumulated in the POM fraction of both growing substrates, while its content in the MAOM was 3 times higher in R70C30 than in S70C30. No significant differences between BK and RH were found. Finally, ferrihydrite mediated exogenous OM stabilization in regolith-based substrates, while Fe(III)-OM complexes were detected exclusively in sand-based growing media. Understanding mechanisms and testing potential sustainable practices for creating Mars regolith similar to terrestrial soil will be fundamental to sustain food crop production on Mars.

Keywords: *Solanum tuberosum*; regolith; MMS-1; compost; MAOM; Fe EXAFS; Fe XANES

check for updates

Citation: Giannetta, B.; Caporale, A.G.; Olivera de Souza, D.; Adamo, P.; Zaccone, C. Evidence of Potential Organo-Mineral Interactions during the First Stage of Mars Terraforming. *Soil Syst.* **2023**, *7*, 92. https://doi.org/10.3390/soilsystems7040092

Academic Editor: Robert White

Received: 27 July 2023
Revised: 24 September 2023
Accepted: 16 October 2023
Published: 20 October 2023

Copyright: © 2023 by the authors. Licensee MDPI, Basel, Switzerland. This article is an open access article distributed under the terms and conditions of the Creative Commons Attribution (CC BY) license (https://creativecommons.org/licenses/by/4.0/).

1. Introduction

Space scientists indifferently used the terms soil and regolith to refer to loose extraterrestrial surfaces. However, it has been lately established that the altered Mars surface deserves the name of soil [1,2]. A major challenge faced by space research studies relates to the possibility to establish a fertile and biologically active substrate to grow edible plants. Long-term manned missions beyond low Earth orbit are dependent on external food supplies and inputs, but making them periodically available is unfeasible, both from the economic and operative point of view. As a consequence, the development of bioregenerative life support systems (BLSS) that are based on the utilization of in situ resources and on recycling organic wastes becomes an imperative [3].

Martian regolith can be described as a fine-grained and cohesionless rocky matrix mixed with dust [4]. It contains plagioclases in mixture with amorphous materials (ca.

20–50%; [5]), zeolite, hematite, and smectite, thus having most of the essential plant nutrients, such as Ca, K, Mg, and Fe [6], but lacking N and organic C [7,8]. Among the strategies possibly applied to overcome the nutrient deficiency of Mars simulants, amendment with compost would allow to offset the lack of organic matter (OM) [9] and represents a valid strategy for recycling inedible crop waste and crew sewage. However, studies based on Mars simulants amendment with compost are quite rare [6,10]. The Mojave Mars Simulant MMS-1 has been applied as a cultivation substrate for different crops (e.g., potato) in BLSS, providing promising results especially when mixed with green compost at the rate of 30% in volume [7,8,11]. At the same time, the potential application of those simulants for agricultural applications needs to be better reveled [12]; in fact, the mineralogical and physical accuracy of these simulants as proxies for Martian sites being under debate, and considering that experiments are carried out on Earth, any conclusion drawn from studies with these simulants has to be considered with some degree of caution [13]. In any case, sustainable and long-term fertility of these regolith simulant-based substrates can only be achieved through an adequate crop rotation (which should include Fabaceae/Leguminosae species) and a constant supply of biomass composted in situ over time, in an almost 'closed-loop system'.

Stabilization mechanisms and turnover of soil organic C under different amendments are dependent on both the amendment rate and quality [14], as well as on their interaction with the mineral matrix, which provides physical and chemical protection against microbial decomposition [15]. A more detailed evaluation of the mechanisms involved in C accrual can be revealed by separating functionally defined OM fractions, i.e., particulate OM (POM) and mineral-associated OM (MAOM) [16].

Identifying sustainable strategies for creating a regolith-based matrix similar to terrestrial soil, where microorganisms and OM interact with mineral surfaces, is the key to sustain food productivity on Mars. In order to test the potential of Mars regolith simulants as a plant growth substrate, they have been characterized for mineralogical, physical, chemical, and hydraulic properties [7,17–20], while no data are available on the potential stabilization of exogeneous OM by minerals, including iron (Fe) (oxyhydr)oxides, over time. Accruing OM in such a mineral matrix is of paramount importance for the survival of crops. The Martian regolith contains phyllosilicates (smectite and saponite), sulphate salts, and Fe oxides (including ferrihydrite, hematite, and magnetite) that make Mars "the red planet" [21]. Organic C stabilization in soils is often promoted by Fe (oxyhydr)oxides, and the interaction between poorly crystalline mineral species and organic C is widely considered as one of the most important mechanisms for C preservation [22–25].

In this study, we would like to address the following research questions: (i) what is the Fe speciation characterizing POM and MAOM fractions during terraforming? (ii) Do Fe mineral species significantly contribute to the stabilization of OM into the different fractions over time? (iii) Do organo-mineral interactions vary in bulk vs. tubero/rhizosphere soil? We hypothesize that the exogenous OM, added in the form of compost, would preferentially occur in the POM fraction during the first months of incubation, while we expect that Fe phases could vary over time in both fractions, promoting the formation of Fe–OM complexes. Providing an answer to these questions will help to identify the main critical aspects and future challenges related to sustainable space farming, which involves the in situ use of Martian resources.

2. Materials and Methods

2.1. Plant Growth Experiment

The experiment was conducted in a cold glasshouse where potato (*Solanum tuberosum* L.) was grown from pre-sprouted mini-tuber seeds. The cultivar 'Colomba' (HZPC Holland B.V.) was selected for cultivation in BLSS due to its small size, short growing cycle, and high productivity; moreover, it was previously tested in controlled environment under different artificial light sources and in microgravity [26,27]. Four substrates were included in this study: the Mojave Mars regolith Simulant (MMS-1), alone (R100) and combined

with a green compost in a ratio 70:30 *v:v* (R70C30), and a fluvial quartz sand, alone (S100) or mixed with compost at the same ratio (S70C30). Each treatment consisted of 3 replicates (pots), randomly distributed. More details about the compost used and the experimental design are reported elsewhere [7,11].

2.2. Sampling and Measurements

At the end of the experiment (i.e., 99 days after mini-tubers sowing) and at the sampling of the aboveground biomass (stems and leaves; [11]), the differently filled pots were gently handled to harvest potato tubers and separate root biomass from the growth media (i.e., R100, R70C30, S100, S70C30). During this phase, soil adhering to potato tubers and plant roots (tubero/rhizo-sphere soil—RH) was collected separately from the bulk soil (BK). Both RH and BK samples were dried at room temperature, gently ground, and then sieved at 2 mm for further analyses.

2.3. Physical Fractionation of OM

All substrates (WHOLE) were size-fractionated after aggregate dispersion, following the method described by Cambardella and Elliott [28]. Briefly, 10.5 g of 2 mm sieved soil were shaken for 18 h in 5 g L^{-1} sodium hexametaphosphate. After dispersion, samples were sieved using a vibratory sieve shaker (AS 200, Retsch, Haan, Germany). POM represented the fraction remaining on the sieve (>53 µm), while MAOM the fraction that passed through it (<53 µm). All fractions were oven-dried at 60 °C, and ground with a zirconium ball mill (MM 400, Retsch) for analyses.

2.4. Organic C, Total N, and Major and Trace Elements Determination

Total C and N contents of bulk substrates and corresponding fractions were determined by dry combustion using an elemental analyzer (CHNS vario MACRO cube, Elementar, Langenselbold, Germany). To determine organic C, all samples underwent acid (HCl) fumigation before analysis to remove carbonates [29].

The total concentration of major (Si, Ca, Fe, Al, K, Na, Mg, P, Mn; g kg^{-1}) and trace (Zn and Cu; mg kg^{-1}) elements was determined in acid-digested bulk samples and fractions by Inductively Coupled Plasma—Optical Emission Spectrometry (ICP-OES, Thermo Scientific iCAP 7400, Waltham, MA, USA). The quality of analyses was monitored using the European Reference Material CRM 141R (calcareous loam soil, Institute for Reference Materials and Measurements, European Commission Joint Research Centre, Geel, Belgium); element recoveries were around ±10% of the certified values. The digestion of samples (100 mg each) was performed in a microwave digestion system (Milestone Start D, Sorisole, Italy), with a blend of HCl 37% (3 mL), HNO_3 65% (1 mL), and HF 39.5% (0.3 mL).

2.5. Fe EXAFS and XANES

X-ray absorption spectroscopic analyses of POM and MAOM fractions were conducted at the XAFS beamline at Elettra Sincrotrone (Trieste, Italy). For each treatment, the 3 replicates were pooled and homogenized to obtain the final samples. Aliquots of ca. 15 mg were powdered, pressed into pellets, fixed with Kapton® tape, and then mounted in a chamber at room temperature. Fe spectra were collected in transmission mode by a Si (111) monochromator and calibrated to the first-derivative maximum of the K-edge absorption spectrum of a metallic Fe foil (7112 eV). The energy used for their acquisition was in the range 6812–7660 eV, with a variable step size and integration time of 2 s per point. Each pellet was measured at least 3 times to check for beam damage on the samples.

The analysis of the XANES pre-edge peak at the Fe K-edge is mainly applied to identify differences in the relative oxidation state among samples. The intensity, shape, and energy position of the XANES relate to the bonding environment of the irradiated Fe atoms (bonding symmetry, coordination type, length to neighboring atoms) [30] and to the oxidation state.

Ferrihydrite, goethite, hematite, maghemite, siderite, purpurite, illite, smectite, nontronite, and chlorite were selected and used as inorganic Fe-bearing standards, whereas Fe(III)-citrate was chosen as an analogue model compound for Fe–OM complexes [31]. Linear combination fitting (LCF) was carried out on the entire XANES spectrum. Moreover, LCF of both k^2 and k^3-weighted Fe EXAFS spectra was completed over a 2–10 $Å^{-1}$ k range. The software Athena was used to process EXAFS data [32]. We paired both EXAFS and XANES LCF analyses assuming that Fe EXAFS is better suited for the quantification of both Fe complexes with OM and Fe oxyhydroxides. Complementary to this information, Fe K-edge XANES reveals the relative contribution of mineral classes and organic compounds with different Fe oxidation states (e.g., Fe oxyhydroxides, Fe sulphides, organic complexes with Fe(II) or Fe(III)) in soils and sediments.

2.6. Data Analysis

Data shown in Tables 1 and 2 were analyzed according to a factorial combination of four substrates (PS) × three different OM fractions (OMF) × two soil types (RB). The analysis of variance was carried out as three-way analysis of variance (ANOVA) using the software package IBM SPSS Statistics v27 (SPSS Inc., Chicago, IL, USA). When needed, the separation of means was performed through Duncan's multiple range test (DMRT) at $p < 0.05$. Data shown in Figures 1–3 were instead analyzed by one-way ANOVA, post hoc test: Fisher's LSD; statistical differences were assumed at $p < 0.05$.

Table 1. Total, organic, and inorganic C, total N concentrations (g kg^{-1}), and C/N ratio in particulate (POM) and mineral-associated organic matter (MAOM) fractions obtained from Mojave Mars regolith Simulant MMS-1, alone (R100) and mixed with a commercial green compost (70:30 *v*:*v*; R70C30), and fluvial sand, alone (S100) and mixed with compost (70:30 *v*:*v*; S70C30). Tubero/rhizo-sphere (RH) and bulk (BK) soils were also separated after the potato plant growth experiment. WHOLE indicates the bulk substrate. Data are expressed as mean values of three replicates ($n = 3$). Substrate (S), OM fraction (OMF), RH vs. BK (RB), and their interactions were compared by three-way ANOVA, Duncan's multiple-range test (* $p < 0.05$; ** $p < 0.01$; *** $p < 0.001$; ns = not significant). Different lowercase letters within each column indicate significant differences ($p < 0.05$).

Experimental Factors	Total C	Organic C	Inorganic C	Total N	C/N
	g kg^{-1}				
R100	1.78 c	0.51 c	1.27 b	*<0.03* c	
S100	14.81 b	0.96 c	13.85 a	*<0.03* c	
R70C30	14.30 b	12.13 b	2.20 b	0.83 a	13.76
S70C30	23.59 a	10.45 a	13.16 a	0.60 b	16.71
Substrate (S)	***	***	***	***	**
WHOLE	22.31 a	11.19 a	11.12 a	0.76 a	14.87 b
POM	17.96 b	6.33 b	11.63 a	0.34 b	18.60 a
MAOM	0.58 c	0.52 c	0.11 b	0.09 c	10.89 c
OM fraction (OMF)	***	***	***	***	***
RH	13.42	5.98	7.45	0.39	14.53
BK	13.82	6.05	7.79	0.38	15.49
RHvs. BK (RB)	*ns*	*ns*	*ns*	*ns*	*ns*
S × OMF	***	*ns*	***	*	**
S × RB	*ns*	*ns*	*ns*	*ns*	*ns*
OMF × RB	*ns*	*ns*	*ns*	*ns*	*ns*
S × OMF × RB	*ns*	*ns*	*ns*	*ns*	*ns*

Table 2. Average concentrations of total Si, Ca, Fe, Al, K, Na, Mg, P, Mn (g kg^{-1}), Zn, and Cu (mg kg^{-1}) in particulate (POM) and mineral-associated organic matter (MAOM) fractions obtained from Mojave Mars regolith Simulant MMS-1, alone (R100) and mixed with a commercial green compost (70:30 *v*:*v*; R70C30), and fluvial sand, alone (S100) and mixed with compost (70:30 *v*:*v*; S70C30). Tubero/rhizo-sphere (RH) and bulk (BK) soils were also separated after the potato plant growth experiment. WHOLE indicates the bulk substrate. Data are expressed as mean values of three replicates (n = 3). Substrate (S), OM fraction (OMF), RH vs. BK (RB), and their interactions were compared by three-way ANOVA, Duncan's multiple-range test (* $p < 0.05$; ** $p < 0.01$; *** $p < 0.001$; ns = not significant). Different lowercase letters within each column indicate significant differences ($p < 0.05$).

Experimental Factors	Si	Ca	Fe	Al	K	Na	Mg	P	Mn	Zn	Cu
	g kg^{-1}									mg kg^{-1}	
R100	234 a	29.0 c	49.9 a	14.6 a	10.3 b	11.4 a	5.0 d	7.5 b	0.96 a	111 a	41.6 b
S100	215 b	64.3 a	18.7 c	7.6 b	10.4 ab	11.6 a	14.4 a	19.7 a	0.73 c	73 c	30.4 c
R70C30	214 b	30.5 c	44.7 b	14.5 a	9.8 b	10.9 ab	5.8 c	7.4 b	0.87 b	113 a	47.7 a
S70C30	186 c	58.9 b	16.8 d	6.5 b	11.4 a	10.2 b	12.5 b	19.0 a	0.65 d	99 b	49.1 a
Substrate (S)	***	***	***	***	*	***	***	***	***	*	**
WHOLE	248 a	42.6 b	33.4 a	9.2 c	10.2 b	7.5 c	9.4	0.99 b	0.78 b	78 b	28.6 b
POM	206 b	48.6 a	33.9 a	11.1 b	9.8 b	8.7 b	9.7	0.96 b	0.83 a	72 b	27.7 b
MAOM	176 c	42.2 b	32.5 b	13.1 a	11.6 a	18.0 a	8.2	41.9 a	0.81 ab	162 a	78.3 a
OM fraction (OMF)	***	**	***	***	*	***	*ns*	***	*	***	***
RH	210	43.7	33	10.9	10.5	10.9	9.0	13.0	0.80	97	41.4
BK	214	45.5	33.6	11.2	10.5	11.2	9.3	13.0	0.81	104	44.4
RH vs. BK (RB)	*ns*	*ns*	*ns*	*ns*	*ns*	*ns*	*	*ns*	*ns*	***	*ns*
S × OMF	***	***	***	***	*ns*	***	***	***	***	***	***
S × RB	*ns*	*ns*	*ns*	*ns*	*ns*	*ns*	*ns*	*ns*	*ns*	**	*ns*
OMF × RB	*ns*	*ns*	*ns*	*ns*	*ns*	*ns*	*ns*	*ns*	*ns*	***	*ns*
S × OMF × RB	*ns*	*ns*	*ns*	*ns*	*ns*	*ns*	*ns*	*ns*	*ns*	*	*ns*

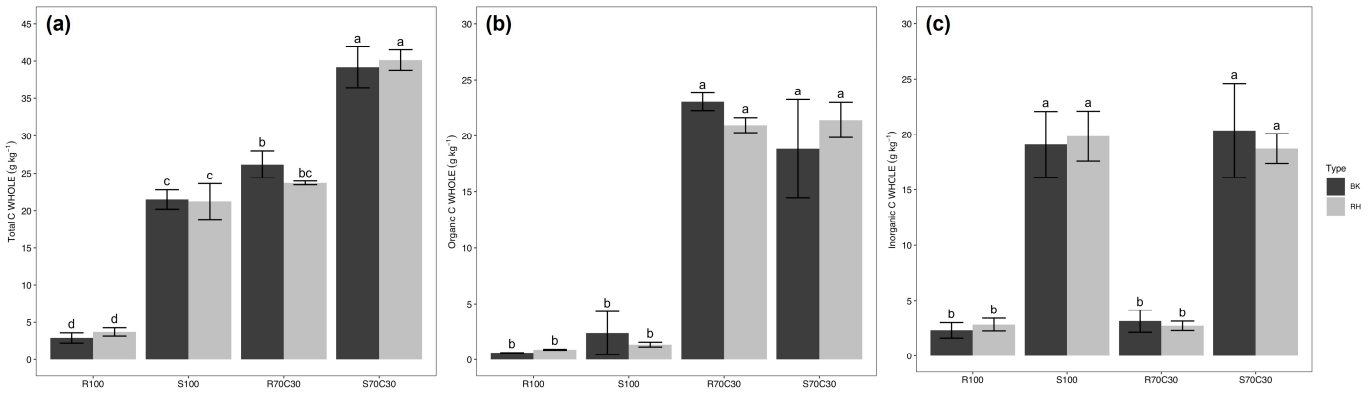

Figure 1. Average concentration (g kg^{-1}) of total (**a**), organic (**b**), and inorganic C (**c**) in WHOLE samples consisting of Mojave Mars regolith Simulant MMS-1, alone (R100) and mixed with a commercial green compost (70:30 *v*:*v*; R70C30), and of fluvial sand, alone (S100) and mixed with compost (70:30 *v*:*v*; S70C30). Tubero/rhizo-sphere (RH) and bulk (BK) soils were also separated after a potato plant growth experiment. WHOLE indicates the bulk substrate. Error bars indicate standard deviation (n = 3). Different lowercase letters indicate statistically significant differences according to Fisher's LSD test at the p = 0.05 level.

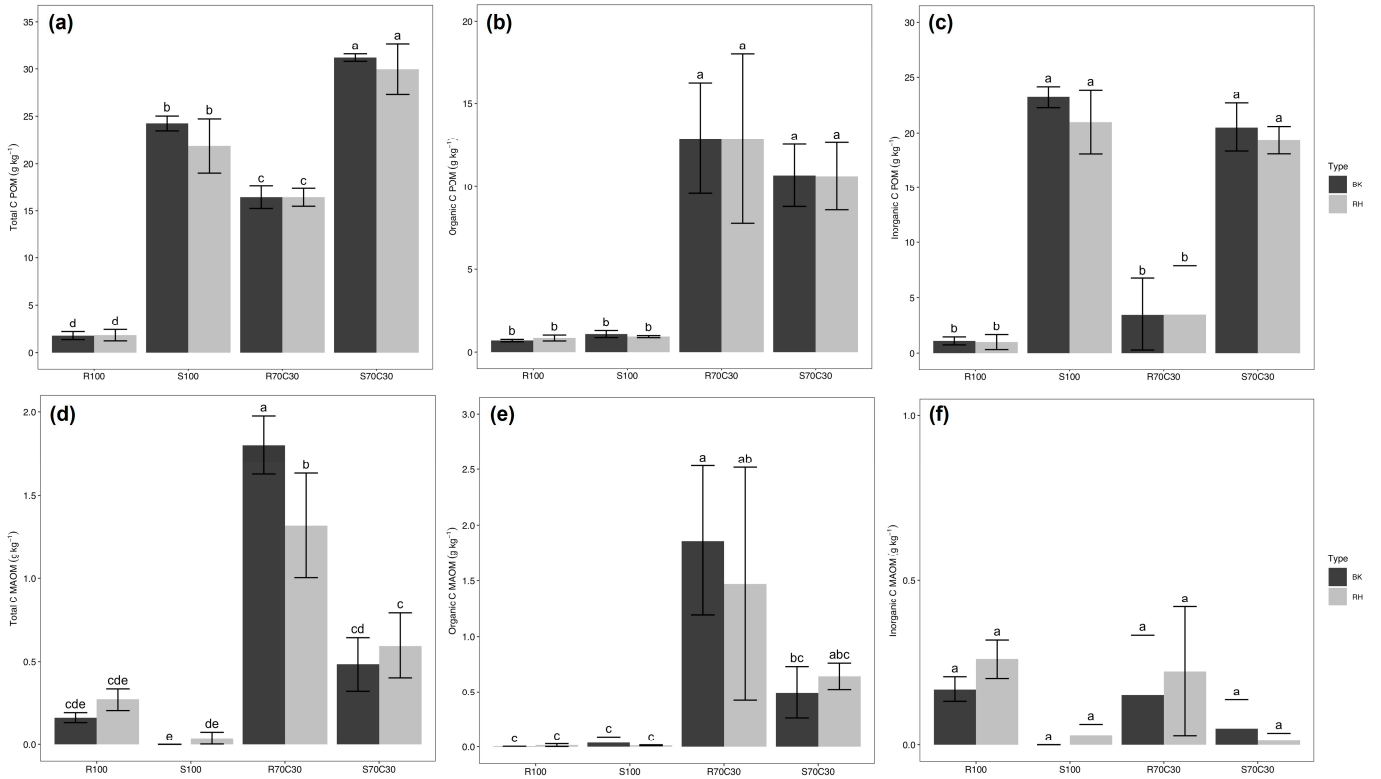

Figure 2. Average concentration (g kg^{-1}) of total, organic, and inorganic C in particulate (POM) (**a**–**c**) and mineral-associated organic matter (MAOM) (**d**–**f**) fractions obtained from Mojave Mars regolith Simulant MMS-1, alone (R100) and mixed with a commercial green compost (70:30 *v*:*v*; R70C30), and fluvial sand, alone (S100) and mixed with compost (70:30 *v*:*v*; S70C30). Tubero/rhizo-sphere (RH) and bulk (BK) soils were also separated after the potato plant growth experiment. Error bars indicate standard deviation (n = 3). Different lowercase letters indicate statistically significant differences according to Fisher's LSD test at the p = 0.05 level.

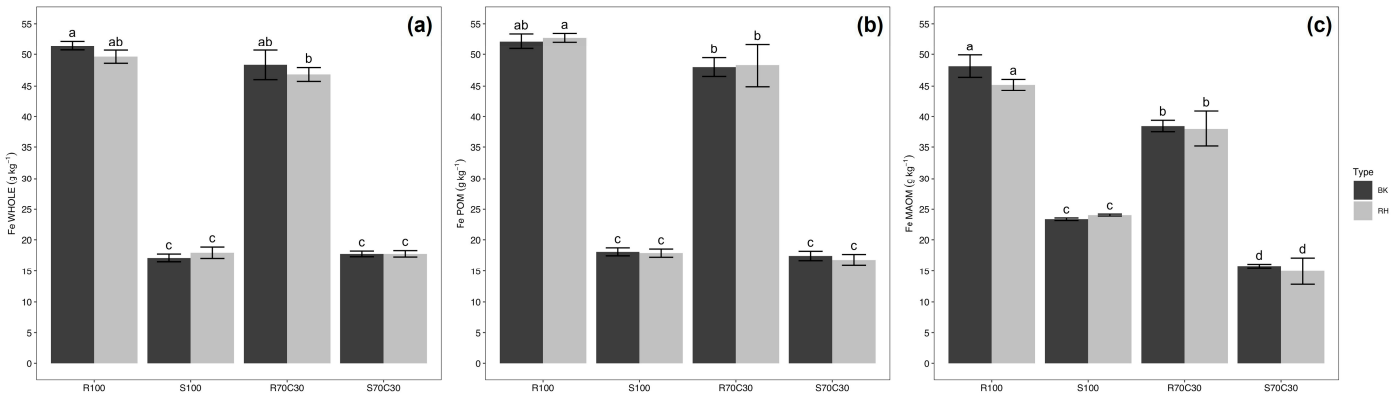

Figure 3. Average concentration (g kg^{-1}) of total Fe in the bulk substrate (WHOLE) (**a**) and in corresponding particulate (POM) (**b**) and mineral-associated organic matter (MAOM) (**c**) fractions. Mojave Mars regolith Simulant MMS-1, alone (R100) and mixed with a commercial green compost (70:30 *v*:*v*; R70C30), and fluvial sand, alone (S100) and mixed with compost (70:30 *v*:*v*; S70C30), were tested. Tubero/rhizo-sphere (RH) and bulk (BK) soils were also separated after the potato plant growth experiment. Error bars indicate standard deviation (n = 3). Different lowercase letters indicate statistically significant differences according to Fisher's LSD test at the p = 0.05 level.

3. Results and Discussion

3.1. Influence of Amendment on C and n Distribution

The total C content (avg ± st.dev.) in the WHOLE substrate ranged from 2.9 ± 0.7 g kg^{-1} in R100 to 40.1 ± 1.4 g kg^{-1} in S70C30 (Figure 1). The amendment with green compost caused a total C increase of ca. 10 times in R70C30 vs. R100, and of ca. 2 times in S70C30 vs. S100 (Table 1; Figure 1).

Thus, compost application significantly affected organic C in both sand and regolith simulant mixtures, although to a different extent (Figure 1b). In fact, an adequate input of composted OM (e.g., 20–30% in volume) in these mineral-based media is crucial to provide energy and nutrients to soil microbiota, promote biological activities, regulate the bioavailability and biogeochemistry of nutrients in the rhizosphere, foster particle interaction and aggregation, and, consequently, enhance soil structure [9]. Inorganic C content was significantly lower in the Martian regolith compared to the fluvial sand, which held a high content of carbonates (Figure 1c; Table 1).

After the fractionation, most of the total and organic C was associated to the POM fraction. In particular, organic C in the POM ranged from 0.8 ± 0.1 g kg^{-1} in R100 to 12.9 ± 3.8 g kg^{-1} in R70C30, and from 1.0 ± 0.2 g kg^{-1} in S100 to 10.7 ± 1.7 g kg^{-1} in S70C30 (Figure 2a–c). In the MAOM fraction, C was present mainly as organic C and exclusively revealed in both the amended substrates (Figure 2d–f), with concentrations ca. 3 times higher in the amended regolith compared to the sand. This implies that, even after only 99 days, the amended regolith can foster the stabilization of exogenous OM by minerals, thus leading to the formation of the MAOM fraction, whose content ranged from 0.9 to 7.5% of the total organic C, in the unamended (R100) and amended regolith simulant (R70C30), respectively. At the same time, the investigated regolith simulant being characterized by a clay plus silt size fraction < 10% [7], the upper limit to the capacity to store organic C could be low; thus, the possibility of a saturation of adsorption sites in the medium to long term needs to be considered.

All fractions were significantly different in terms of total, organic, and inorganic C concentrations ($p < 0.001$); a similar pattern was observed also among the substrates (total and inorganic C, $p < 0.001$; organic C, $p < 0.01$). In contrast, no significant differences were observed for organic C in BK vs. RH soils (Table 1). Total N was quantifiable only in the amended regolith and sand substrates. Overall, the type of substrate (fluvial sand vs. regolith simulant), OM fractions, and their interaction positively affected total N content (Table 1). Following the amendment, the C/N ratio was higher in the POM (20.0 ± 5.3) rather than the MAOM fraction (10.9 ± 2.8); moreover, while both MAOM fractions showed a similar C/N ratio, that of the POM was significantly higher in S70C30 (24.0 ± 1.8) compared to R70C30 (15.8 ± 4.2). No significant differences were observed for the C/N ratio in BK vs. RH soils (Table 1).

3.2. Major and Trace Elements Concentration

Table 2 summarizes the concentrations of major (g kg^{-1}) and trace (mg kg^{-1}) elements in the WHOLE substrate and in both POM and MAOM fractions.

Overall, the MMS-1, alone or combined with compost, was particularly enriched Fe (2.5×) and Al (2×) compared to the fluvial sand, revealing significant differences between substrates and between fractions. Iron concentration was higher in the R100 compared to R70C30, and ca. 2.8 times lower in both S100 and S70C30 (Table 2; Figure 3). The differences between the Fe concentration in the POM fraction of S100 and S70C30 were not significant, whereas the Fe concentration was lower in the POM fraction of the amended simulant (R70C30) and in the MAOM fraction from both amended sand and regolith simulant (Table 2; Figure 3).

Conversely, compared to R100, S100 contained 2× and 3× higher Ca and Mg concentrations, respectively. Both elements were mainly found in the POM fraction.

As expected, the P concentration was lower in the regolith simulant (7.5 g kg^{-1}) compared to the fluvial sand (19 g kg^{-1}). Zn was always higher in the MMS-1, either alone

or amended with compost, while Cu increased after compost addition in both fluvial sand and regolith simulant. Compared to the POM, the MAOM was particularly enriched in Na (18 vs. 8.7 g kg^{-1}), P (41.9 vs. 0.96 g kg^{-1}), Zn (162 vs. 72.3 mg kg^{-1}), and Cu (78.3 vs. 27.7 mg kg^{-1}).

Overall, the differences between the fractions in terms of element concentrations were always significant, with the only exception of Mg. Conversely, no significant differences were found between bulk and tubero/rhizo-sphere soil, with the only exceptions being Mg ($p < 0.05$) and Zn ($p < 0.001$), showing slightly higher concentrations in BK compared to RH.

3.3. Fe EXAFS and XANES LCF

LCF was applied to the normalized Fe K-edge XANES spectra (Table 3), with Fe phases adequately described using four components.

Table 3. Results of LCF performed on the Fe K-edge XANES data of particulate (POM) and mineral-associated organic matter (MAOM) fractions obtained from Mojave Mars regolith Simulant MMS-1, alone (R100) and mixed with a commercial green compost (70:30 *v*:*v*; R70C30), and fluvial sand, alone (S100) and mixed with compost (70:30 *v*:*v*; S70C30). Tubero/rhizo-sphere (RH) and bulk (BK) soils were also separated after the potato plant growth experiment.

	Component 1	(%)	Component 2	(%)	Component 3	(%)	Component 4	(%)
R100 BK POM	Smectite	38	Maghemite	20	Hematite	19	Ferrihydrite	23
R100 RH POM	Smectite	44	Maghemite	15	Hematite	17	Ferrihydrite	24
R100 BK MAOM	Smectite	45	Maghemite	22	Nontronite	3	Ferrihydrite	30
R100 RH MAOM	Smectite	35	Maghemite	20	Nontronite	9	Ferrihydrite	36
R70C30 BK POM	Smectite	31	Maghemite	17	Hematite	20	Ferrihydrite	32
R70C30 RH POM	Smectite	33	Maghemite	19	Hematite	21	Ferrihydrite	27
R70C30 BK MAOM	Smectite	51	Maghemite	21	-		Ferrihydrite	28
R70C30 RH MAOM	Smectite	34	Maghemite	26	Nontronite	10	Ferrihydrite	30
S100 BK POM	Chlorite	58	Smectite	23	Goethite	6	Siderite	13
S100 RH POM	Chlorite	81	-		Goethite	16	Siderite	3
S100 BK MAOM	Chlorite	57	Smectite	7	Goethite	36	-	
S100 RH MAOM	Chlorite	55	Smectite	7	Goethite	38	-	
S70C30 BK POM	Chlorite	74	Siderite	4	Goethite	13	Fe(III)-OM	9
S70C30 RH POM	Chlorite	74	Siderite	4	Goethite	14	Fe(III)-OM	8
S70C30 BK MAOM	Chlorite	33	Smectite	41	Goethite	24	Fe(III)-OM	2
S70C30 RH MAOM	Chlorite	32	Smectite	41	Goethite	15	Fe(III)-OM	12

According to the LCF results, MMS-1 Simulant was characterized mainly by the presence of smectite (31–51%), confirming the X-ray diffraction data of fine particles reported in Caporale et al. [7].

Actually, the presence of smectite deposits on parts of ancient Mars surfaces was also revealed by remotely sensed data [33]. Hematite was found in the POM fraction of both unamended and amended regolith simulants, whereas nontronite was only found in the MAOM fractions. Clay minerals were identified on Mars by orbiter-based spectroscopic analyses, and the presence of smectites (nontronite and montmorillonite) was detected by the OMEGA instrument onboard the European Space Agency (ESA) Mars Express [34]. Fe-rich smectites, including nontronites, are characteristic of the alteration in mafic material such as gabbro or basalt, which are common on Mars [33]. Maghemite (from 15 to 26%) and ferrihydrite (from 23 to 36%) occurred in all fractions and independently from the amendment. Ferrihydrite, a common precursor of hematite and goethite, is the most frequent crystalline Fe(III) oxide occurring in soils. Ferrihydrite precipitated in the presence of phosphate or other ligands can partly transform upon aging into maghemite at 150 °C. This maghemite represents a transient phase in the transformation of ferrihydrite to hematite, and this pathway could partly explain its occurrence in different Earth soils and on the surface of Mars [35,36].

Unlike regolith simulant, all fluvial sand fractions were mainly characterized by the presence of chlorite (from 32 to 81%), goethite (from 6 to 38%), and smectite. Siderite was only occurring in the POM fraction of the fluvial sand, alone or mixed with green compost,

whereas Fe(III) complexed with OM (Fe(III)-OM; 2-12%) was found exclusively in both POM and MAOM from the amended sands.

The EXAFS LCF data were conducted at both k^3 (Table 4; Figure S1) and k^2 (Table 5). In the MAOM fraction of both R100 and R70C30, the presence of nontronite (22–29%) was revealed. EXAFS LCF allowed a better discrimination of the Fe (oxyhydr)oxides. Hematite represented an important mineral phase of both POM and MAOM fractions (29–42%), and, if considering the pure and amended POM fractions, its percentage reached double values compared to the XANES LCF data. Meanwhile, ferrihydrite presence was also revealed using XANES LCF (23–36%); its content detected by EXAFS k^3 LCF was much higher (34–51%), thus confirming that Fe EXAFS can be more suitable to quantify specific Fe oxyhydroxides rather than XANES [37,38]. Traces of siderite were only found in the MAOM fraction. Confirming the XANES data, chlorite represented the main phase of the sand substrate and corresponding fractions. Here, considering the Fe oxide phases, ferrihydrite was found in addition to hematite, only in the POM fraction, and goethite, in the MAOM. Fe(III)-OM percentage was double in both S100 and S70C30 MAOM compared to the POM. In addition, the MAOM fractions of S70C30 contained Fe(III)-OM percentages almost double compared to S100 (Table 4).

Table 4. Results of LCF performed on the Fe K-edge EXAFS (k^3) data of particulate (POM) and mineral-associated organic matter (MAOM) fractions obtained from Mojave Mars regolith Simulant MMS-1, alone (R100) and mixed with a commercial green compost (70:30 *v:v*; R70C30), and fluvial sand, alone (S100) and mixed with compost (70:30 *v:v*; S70C30). Tubero/rhizo-sphere (RH) and bulk (BK) soils were also separated after the potato plant growth experiment.

	Component 1	(%)	Component 2	(%)	Component 3	(%)	Component 4	(%)
R100 BK POM	Illite	9	Hematite	40	Maghemite	7	Ferrihydrite	44
R100 RH POM	Illite	11	Hematite	40	Maghemite	8	Ferrihydrite	41
R100 BK MAOM	Nontronite	29	Hematite	30	Siderite	7	Ferrihydrite	34
R100 RH MAOM	Illite	29	Hematite	25	Siderite	6	Ferrihydrite	40
R70C30 BK POM	Illite	7	Hematite	42	-		Ferrihydrite	51
R70C30 RH POM	Illite	10	Hematite	42	-		Ferrihydrite	48
R70C30 BK MAOM	Nontronite	22	Hematite	30	Siderite	6	Ferrihydrite	42
R70C30 RH MAOM	Nontronite	23	Hematite	29	Siderite	6	Ferrihydrite	42
S100 BK POM	Chlorite	55	Hematite	9	Ferrihydrite	22	Fe(III)-OM	14
S100 RH POM	Chlorite	56	Hematite	10	Ferrihydrite	24	Fe(III)-OM	10
S100 BK MAOM	Chlorite	52	Goethite	20	Siderite	4	Fe(III)-OM	24
S100 RH MAOM	Chlorite	50	Goethite	22	Siderite	3	Fe(III)-OM	25
S70C30 BK POM	Chlorite	54	Hematite	7	Ferrihydrite	23	Fe(III)-OM	16
S70C30 RH POM	Chlorite	53	Hematite	6	Ferrihydrite	20	Fe(III)-OM	21
S70C30 BK MAOM	Chlorite	36	Goethite	11	Ferrihydrite	11	Fe(III)-OM	42
S70C30 RH MAOM	Chlorite	40	Goethite	10	Ferrihydrite	16	Fe(III)-OM	34

Therefore, after 99 days, the addition of OM increased the capability of the fluvial sand to stabilize organic C, mainly through the formation of Fe(III)-OM complexes. Adding exogenous OM might increase the specific surface area (SSA) of sand particles by newly formed Fe surface coatings [23,39]. In fact, Scheidegger et al. [40] reported increased SSA in silica sand after reaction with Fe(III) oxides, while Penn et al. [41] provided evidence about the sorption of Fe(III) onto quartz surfaces and the formation of Fe oxide minerals, where coatings dominated the reactive SSA.

Conversely, in the regolith simulant mixture, the interaction with freshly added amendments can lead to surface site blockage and to the formation of aggregates and thus to a lower dissolution of ferrihydrite [23]. Consequently, ferrihydrite could represent the next potential stabilizing agent of exogenous OM in regolith simulant, although coating processes, like those observed for the fluvial sand, could not be excluded in the medium to long term.

Few differences were revealed only in the regolith substrate comparing the LCF of k^3 and the k^2-weighted Fe K-edge EXAFS spectra. Aside from traces of siderite found in the MAOM fraction, in the POM, purpurite was also detected (Table 5).

Table 5. Results of LCF performed on the Fe K-edge EXAFS (k^2) data of particulate (POM) and mineral-associated organic matter (MAOM) fractions obtained from Mojave Mars regolith Simulant MMS-1, alone (R100) and mixed with a commercial green compost (70:30 *v:v*; R70C30), and fluvial sand, alone (S100) and mixed with compost (70:30 *v:v*; S70C30). Tubero/rhizo-sphere (RH) and bulk (BK) soils were also separated after the potato plant growth experiment.

	Component 1	(%)	Component 2	(%)	Component 3	(%)	Component 4	(%)
R100 BK POM	Illite	2	Hematite	41	Purpurite	10	Ferrihydrite	47
R100 RH POM	Nontronite	9	Hematite	44	-		Ferrihydrite	47
R100 BK MAOM	Nontronite	29	Hematite	30	Siderite	7	Ferrihydrite	34
R100 RH MAOM	Nontronite	25	Hematite	32	Siderite	5	Ferrihydrite	38
R70C30 BK POM	Illite	6	Hematite	41	Purpurite	4	Ferrihydrite	45
R70C30 RH POM	Illite	10	Hematite	38	Maghemite	13	Ferrihydrite	40
R70C30 BK MAOM	Nontronite	25	Hematite	31	Siderite	5	Ferrihydrite	39
R70C30 RH MAOM	Nontronite	24	Hematite	31	Siderite	5	Ferrihydrite	40
S100 BK POM	Chlorite	53	Hematite	8	Ferrihydrite	22	Fe(III)-OM	17
S100 RH POM	Chlorite	54	Hematite	10	Ferrihydrite	24	Fe(III)-OM	12
S100 BK MAOM	Chlorite	50	Goethite	16	Siderite	13	Fe(III)-OM	21
S100 RH MAOM	Chlorite	52	Goethite	20	Siderite	4	Fe(III)-OM	24
S70C30 BK POM	Chlorite	52	Hematite	8	Ferrihydrite	25	Fe(III)-OM	15
S70C30 RH POM	Chlorite	50	Maghemite	21	Ferrihydrite	5	Fe(III)-OM	24
S70C30 BK MAOM	Chlorite	40	Goethite	13	Ferrihydrite	16	Fe(III)-OM	31
S70C30 RH MAOM	Chlorite	40	Goethite	13	Ferrihydrite	16	Fe(III)-OM	31

4. Conclusions

While Mars regolith simulants have been widely characterized to test their potential as plant growth substrates, the stabilization of exogeneous OM by minerals, including Fe oxides, over time still needs to be unraveled. This aspect is of paramount importance as it regulates the accrual of OM in this mineral matrix, thus allowing the optimal cultivation and the survival of crops in long-term space missions.

Particulate organic C ranged from 0.8 in R100 to 12.9 g kg^{-1} in R70C30, and from 1 in S100 to 10.7 g kg^{-1} in S70C30. Most of the total C in the MAOM fraction was organic and exclusively revealed in both the amended substrates, with the organic C content ca. 3 times higher in the amended regolith compared to the fluvial sand. This implies that, even after 99 days, the amended regolith simulant can sustain stabilization of exogenous OM by minerals, promoting the formation of the MAOM fraction. No significant differences were observed in terms of organic C content in BK vs. RH soil.

Fe EXAFS data revealed the presence of different Fe oxides; in detail, ferrihydrite content was double in the EXAFS, compared to XANES, for the regolith, whereas Fe(III) complexed with OM was only found in the amended sands, in both POM and MAOM. In the MAOM fraction, the amended sand contained Fe(III)-OM percentages almost double the pure one. Therefore, in the short term, ferrihydrite mediates exogenous OM stabilization in MMS-1, while Fe(III)-OM complexes in sand.

This study represents the first knowledge on the formation of organo-mineral complexes in Martian regolith-based substrates able to sustain food crop production. Further studies with other candidate crop species, including Fabaceae species (likely a complete crop rotation), grown on the substrates retrieved after potato cultivation, are currently ongoing to investigate processes, mechanisms, possible limitations (e.g., saturation of adsorption sites for C), and potential sustainable practices for creating Mars regolith akin to terrestrial soil, allowing to stabilize OM in the medium to long term.

Supplementary Materials: The following supporting information can be downloaded at: https://www.mdpi.com/article/10.3390/soilsystems7040092/s1. Figure S1: Fe K-edge EXAFS k3-weighted spectra of particulate (POM) and mineral-associated organic matter (MAOM) fractions obtained from Mojave Mars regolith Simulant MMS-1, alone (R100) and mixed with a commercial green compost (70:30 *v:v*; R70C30) (a), and fluvial sand, alone (S100) and mixed with compost (70:30 *v:v*; S70C30) (b). Tubero/rhizo-sphere (RH) and bulk (BK) soils were also separated after the potato plant growth experiment. Empty circles indicate the sample data, whereas red lines represent the fit. R-factors are also displayed in parenthesis.

Author Contributions: B.G.: Conceptualization, Investigation, Methodology, Validation, Writing—original draft, Writing—review and editing.; A.G.C.: Conceptualization, Formal analysis, Investigation, Methodology, Writing—review and editing.; D.O.d.S.: Formal analysis, Investigation, Validation, Writing—review and editing.; P.A.: Conceptualization, Funding acquisition, Methodology, Supervision, Writing—review and editing.; C.Z.: Conceptualization, Funding acquisition, Investigation, Methodology, Resources, Supervision, Writing—original draft, Writing—review and editing. All authors have read and agreed to the published version of the manuscript.

Funding: This work was partially supported by the Italian Space Agency (ASI)—Project Rebus: In situ resource bio-utilization for life support system (CUP F74I16000000005).

Data Availability Statement: Not applicable.

Acknowledgments: Authors thank the Laboratory of Multielement Analyses (LAM) of the Department of Agricultural Sciences, University of Naples Federico II (Portici, Italy), a lab facility included in the frame of METROFOOD-IT (NextGenerationEU, PNRR-M2C4I3.1, DM 120 21/06/2022, IR0000033), and the instrument leader Diana Agrelli for the expertise and valuable support in the ICP-OES analyses.

Conflicts of Interest: The authors declare no conflict of interest.

References

1. Certini, G.; Scalenghe, R. Do soils exist outside Earth? *Planet. Space Sci.* **2010**, *58*, 1767–1770. [CrossRef]
2. Certini, G.; Karunatillake, S.; Zhao, Y.Y.S.; Meslin, P.Y.; Cousin, A.; Hood, D.R.; Scalenghe, R. Disambiguating the soils of Mars. *Planet. Space Sci.* **2020**, *186*, 104922. [CrossRef]
3. Häder, D.P.; Braun, M.; Hemmersbach, R. Bioregenerative Life Support Systems in Space Research. In *Gravitational Biology I*; Springer Briefs in Space Life Sciences; Springer: Cham, Switzerland, 2018; pp. 113–122.
4. Peters, G.H.; Abbey, W.; Bearman, G.H.; Mungas, G.S.; Smith, J.A.; Anderson, R.C.; Douglas, S.; Beegle, L.W. Mojave Mars simulant—Characterization of a new geologic Mars analog. *Icarus* **2008**, *197*, 470–479. [CrossRef]
5. Rampe, E.B.; Ming, D.W.; Blake, D.F.; Bristow, T.F.; Chipera, S.J.; Grotzinger, J.P.; Morris, R.V.; Morrison, S.M.; Vaniman, D.T.; Yen, A.S.; et al. Mineralogy of an ancient lacustrine mudstone succession from the Murray formation, Gale crater, Mars. *Earth Planet. Sci. Lett.* **2017**, *471*, 172–185. [CrossRef]
6. Wamelink, G.W.W.; Frissel, J.Y.; Krijnen, W.H.J.; Verwoert, M.R.; Goedhart, P.W. Can plants grow on Mars and the Moon: A growth experiment on Mars and Moon soil simulants. *PLoS ONE* **2014**, *9*, 103138. [CrossRef] [PubMed]
7. Caporale, A.G.; Vingiani, S.; Palladino, M.; El-Nakhel, C.; Duri, L.; Pannico, A.; Rouphael, Y.; De Pascale, S.; Adamo, P. Geo-mineralogical characterisation of Mars simulant MMS-1 and appraisal of substrate physico-chemical properties and crop performance obtained with variable green compost amendment rates. *Sci. Total Environ.* **2020**, *720*, 137543. [CrossRef]
8. Duri, L.G.; El-Nakhel, C.; Caporale, A.G.; Ciriello, M.; Graziani, G.; Pannico, A.; Palladino, M.; Ritieni, A.; De Pascale, S.; Vingiani, S.; et al. Mars Regolith simulant ameliorated by compost as in situ cultivation substrate improves lettuce growth and nutritional aspects. *Plants* **2020**, *9*, 628. [CrossRef]
9. Duri, L.G.; Caporale, A.G.; Rouphael, Y.; Vingiani, S.; Palladino, M.; De Pascale, S.; Adamo, P. The potential for lunar and martian regolith simulants to sustain plant growth: A multidisciplinary overview. *Front. Astron. Space Sci.* **2022**, *8*, 747821. [CrossRef]
10. Mortley, D.G.; Aglan, H.A.; Bonsi, C.K.; Hill, W.A. *Growth of sweetpotato in Lunar and Mars Simulants*; SAE Technical Paper 2000-01-2289; SAE: Warrendale, PA, USA, 2000.
11. Caporale, A.G.; Paradiso, R.; Luizzi, G.; Palladino, M.; Amitrano, C.; Arena, C.; Arouna, N.; Verrillo, M.; Cozzolino, V.; De Pascale, S. Green compost amendment improves potato plant performance on Mars regolith simulant as substrate for cultivation in space. *Plant Soil* **2023**, *486*, 217–233. [CrossRef]
12. Fackrell, L.E.; Schroeder, P.A.; Thompson, A.; Stockstill-Cahill, K.; Hibbitts, C.A. Development of martian regolith and bedrock simulants: Potential and limitations of martian regolith as in-situ resource. *Icarus* **2021**, *354*, 114055. [CrossRef]
13. Eichler, A.; Hadland, N.; Pickett, D.; Masaitis, D.; Handy, D.; Perez, A.; Batcheldor, D.; Wheeler, B.; Palmer, A. Challenging the agricultural viability of martian regolith simulants. *Icarus* **2021**, *354*, 114022. [CrossRef]
14. Sonsri, K.; Naruse, H.; Watanabe, A. Mechanisms controlling the stabilization of soil organic matter in agricultural soils as amended with contrasting organic amendments: Insights based on physical fractionation coupled with ^{13}C NMR spectroscopy. *Sci. Total Environ.* **2022**, *825*, 153853. [CrossRef] [PubMed]
15. Six, J.; Conant, R.T.; Paul, E.A.; Paustian, K. Stabilization mechanisms of soil organic matter: Implications for C-saturation of soils. *Plant Soil* **2002**, *241*, 155–176. [CrossRef]
16. Rocci, K.S.; Lavallee, J.M.; Stewart, C.E.; Cotrufo, M.F. Soil organic carbon response to global environmental change depends on its distribution between mineral-associated and particulate organic matter: A meta-analysis. *Sci. Total Environ.* **2021**, *793*, 1459–148569. [CrossRef]
17. Perko, H.A.; Nelson, J.D.; Green, J.R. Mars Soil Mechanical Properties and Suitability of Mars Soil Simulants. *J. Aerosp. Eng.* **2006**, *19*, 169–176. [CrossRef]

18. Ehlmann, B.L.; Edwards, C.S. Mineralogy of the martian surface. *Annu. Rev. Earth Planet. Sci.* **2014**, *42*, 291–315. [CrossRef]
19. Delage, P.; Karakostas, F.; Dhemaied, A.; Belmokhtar, M.; Lognonné, P.; Golombek, M.; De Laure, E.; Hurst, K.; Dupla, J.C.; Kedar, S.; et al. An Investigation of the Mechanical Properties of Some Martian Regolith Simulants with Respect to the Surface Properties at the InSight Mission Landing Site. *Space Sci. Rev.* **2017**, *211*, 191–213. [CrossRef]
20. Kasyap, S.S.; Senetakis, K. A Grain-Scale Study of Mojave Mars Simulant (MMS-1). *Sensors* **2021**, *21*, 4730. [CrossRef]
21. Ramkissoon, N.K.; Pearson, V.K.; Schwenzer, S.P.; Schröder, C.; Kirnbauer, T.; Wood, D.; Seidel, R.G.W.; Miller, M.A.; Olsson-Francis, K. New simulants for martian regolith: Controlling iron variability. *Planet. Space Sci.* **2019**, *179*, 10472. [CrossRef]
22. Lalonde, L.; Mucci, A.; Ouellet, A.; Gélinas, Y. Preservation of organic matter in sediments promoted by iron. *Nature* **2012**, *483*, 198–200. [CrossRef]
23. Giannetta, B.; Plaza, C.; Siebecker, M.G.; Aquilanti, G.; Vischetti, C.; Plaisier, J.; Juanco, M.; Sparks, D.L.; Zaccone, C. Iron speciation in organic matter fractions isolated from soils amended with biochar and organic fertilizers. *Environ. Sci. Technol.* **2020**, *54*, 5093–5101. [CrossRef]
24. Giannetta, B.; Siebecker, M.G.; Zaccone, C.; Plaza, C.; Rovira, P.; Vischetti, C.; Sparks, D.L. Iron(III) fate after complexation with soil organic matter in fine silt and clay fractions: An EXAFS spectroscopic approach. *Soil Till. Res.* **2020**, *200*, 104617. [CrossRef]
25. Giannetta, B.; Plaza, C.; Thompson, A.; Plante, A.F.; Zaccone, C. Iron speciation in soil size fractions under different land uses. *Geoderma* **2022**, *418*, 115842. [CrossRef]
26. Paradiso, R.; Arena, C.; Rouphael, Y.; d'Aquino, L.; Makris, K.; Vitaglione, P.; De Pascale, S. Growth, photosynthetic activity and tuber quality of two potato cultivars in controlled environment as affected by light source. *Plant Biosyst.* **2019**, *153*, 725–735. [CrossRef]
27. Paradiso, R.; Ceriello, A.; Pannico, A.; Sorrentino, S.; Palladino, M.; Giordano, M.; Fortezza, R.; De Pascale, S. Design of a module for cultivation of tuberous plants in microgravity: The ESA Project "Precursor of Food Production Unit" (PFPU). *Front. Plant Sci.* **2020**, *11*, 417. [CrossRef]
28. Cambardella, C.A.; Elliott, E.T. Particulate Soil Organic-Matter Changes across a Grassland Cultivation Sequence. *Soil Sci. Soc. Am. J.* **1992**, *56*, 777–783. [CrossRef]
29. Harris, D.; Horwath, W.R.; van Kessel, C. Acid fumigation of soils to remove carbonates prior to total organic carbon or carbon-13 isotopic analysis. *Soil Sci. Soc. Am. J.* **2001**, *65*, 1853–1856. [CrossRef]
30. Wilke, M.; Farges, F.; Petit, P.-E.; Brown, G.E.; Martin, F. Oxidation state and coordination of Fe in minerals: An Fe K-XANES spectroscopic study. *Am. Mineral.* **2001**, *86*, 714–730. [CrossRef]
31. O'Day, P.A.; Rivera, N.; Root, R.; Carroll, S.A. X-ray absorption spectroscopic study of Fe reference compounds for the analysis of natural sediments. *Am. Mineral.* **2004**, *89*, 572–585. [CrossRef]
32. Ravel, B.; Newville, M. ATHENA, ARTEMIS, HEPHAESTUS: Data analysis for X-ray absorption spectroscopy using IFEFFIT. *J. Synchrotron Radiat.* **2005**, *12*, 537–541. [CrossRef]
33. Poulet, F.; Bibring, J.-P.; Mustard, J.F.; Gendrin, A.; Mangold, N.; Langevin, Y.; Arvidson, R.E.; Gondet, B.; Gomez, C.; the Omega Team. Phyllosilicates on Mars and implications for early martian climate. *Nature* **2005**, *438*, 623–627. [CrossRef]
34. Mustard, J.F.; Murchie, S.L.; Pelkey, S.M.; Ehlmann, B.L.; Milliken, R.E.; Grant, J.A.; Bibring, J.P.; Poulet, F.; Bishop, J.; Dobrea, E.N.; et al. Hydrated silicate minerals on Mars observed by the Mars Reconnaissance Orbiter CRISM instrument. *Nature* **2008**, *454*, 305–309. [CrossRef] [PubMed]
35. Torrent, J.; Barrón, V. Key Role of Phosphorus in the Formation of the Iron Oxides in Mars Soils? *Icarus* **2000**, *145*, 645–647. [CrossRef]
36. Barrón, V.; Torrent, J. Evidence for a simple pathway to maghemite in Earth and Mars soils. *Geochim. Cosmochim. Acta* **2002**, *66*, 2801–2806. [CrossRef]
37. Giannetta, B.; Oliveira de Souza, D.; Aquilanti, G.; Celi, L.; Said-Pullicino, D. Redox-driven changes in organic C stabilization and Fe mineral transformations in temperate hydromorphic soils. *Geoderma* **2022**, *406*, 115532. [CrossRef]
38. Giannetta, B.; Cassetta, M.; Oliveira de Souza, D.; Mariotto, G.; Aquilanti, G.; Zaccone, C. Coupling X-ray absorption and Raman spectroscopies to characterize iron species in a karst pedosedimentary record. *Soil Syst.* **2022**, *6*, 24. [CrossRef]
39. Giannetta, B.; Zaccone, C.; Plaza, C.; Siebecker, M.G.; Rovira, P.; Vischetti, C.; Sparks, D.L. The role of Fe(III) in soil organic matter stabilization in two size fractions having opposite features. *Sci. Total Environ.* **2019**, *653*, 667–674. [CrossRef]
40. Scheidegger, A.; Borkovec, M.; Sticher, H. Coating of silica sand with goethite: Preparation and analytical identification. *Geoderma* **1993**, *58*, 43–65. [CrossRef]
41. Penn, R.L.; Zhu, C.; Xu, H.; Veblen, D.R. Iron oxide coatings on sand grains from the Atlantic coastal plain: High-resolution transmission electron microscopy characterization. *Geology* **2001**, *29*, 843–846. [CrossRef]

Disclaimer/Publisher's Note: The statements, opinions and data contained in all publications are solely those of the individual author(s) and contributor(s) and not of MDPI and/or the editor(s). MDPI and/or the editor(s) disclaim responsibility for any injury to people or property resulting from any ideas, methods, instructions or products referred to in the content.